Rock Mech. Rock Engng. (2008) 41 (1), 59–84
DOI 10.1007/s00603-007-0143-x
Printed in The Netherlands

Rock Mechanics and Rock Engineering

Results of Back-Analysis of the Propagation of Rock Avalanches as a Function of the Assumed Rheology

By

M. Pirulli[1] and **A. Mangeney**[2,3]

[1] Department of Structural and Geotechnical Engineering, Politecnico di Torino, Torino, Italy
[2] Equipe de Sismologie, Institut de Physique du Globe de Paris, Université Denis Diderot, Paris, France
[3] Now at Institut for Nonlinear Science, University of California San Diego, La Jolla, USA

Received September 12, 2006; accepted March 12, 2007
Published online June 21, 2007

Summary

Numerical simulation can provide a useful tool for investigating the dynamics of phenomena like rock avalanches, within realistic geological contexts and in the framework of a better risk assessment and decision making. Difficulties in numerical modelling of a heterogeneous moving mass are mainly linked to the simulation of the complex behaviour assumed by the mass during propagation.

The numerical code RASH3D, based on a continuum mechanics approach and on the long wave approximation, is used to back-analyse two cases of rock avalanches: Frank (1903, Canada) and Val Pola (1987, Italy). The two events are characterised by approximately the same volume (about $30 \times 10^6\,m^3$) while the run out area morphologies are widely different.

Three alternative "rheologies" (Frictional, Voellmy and Pouliquen) are used. Comparison among obtained results underlines that the validation of a "rheology" requires not only a good agreement between the numerical simulation results and the run out area boundaries but also in term of depth distribution of the mass in the deposit.

In case of a Frictional rheology, the obtained calibrated dynamic friction angle values are in a range of $15 \pm 1^\circ$ for both the cases; while assuming a Pouliquen or a Voellmy rheology it emerges a different behaviour of rheological parameters for each of the considered events.

Besides the calibration of rheological parameters to better back-analyse each of the considered events, it is investigated how the behaviour due to the assumed rheology is influenced by the geometry of the run out area (e.g. narrow or broad valley).

Keywords: Rock avalanche, continuum mechanics, back-analysis, rheology, local morphology.

1. Introduction

Rock avalanches are uncommon, large, catastrophic events in which rock fragments, originated from a large rock slide or rock fall, move in a massive way at high speeds as

a semi-coherent flowing mass. The source material can be any kind of rock, sedimentary, metamorphic or igneous, including pyroclastic deposits (Hungr et al., 2001).

Due to an increased development of mountainous areas, human settlements are bringing more and more within reach of landslide hazards. Since it often proves impossible to mitigate the destructive potential of this type of events by stabilising the area of origin, reliable predictions of run out could help to reduce losses, to estimate the extension of the hazardous areas and to avoid exceedingly conservative decisions regarding the development of an area.

The comprehension of the mechanism initiating a rock avalanche is outside the scope of this paper. It is here assumed that the mass has lost its equilibrium and attention is focused on the analysis of the run out phase, which includes the downslope movement and stopping of the mass.

First early methods for rock avalanche run out prediction concerned simple empirical correlations among historical data (e.g. Scheidegger, 1973; Hsu, 1975; Li, 1983; Davies, 1982; Nicoletti and Sorriso Valvo, 1991). Nowadays, analytical and numerical prediction methods are receiving an increased attention from the researchers.

In the continuum mechanics context, Savage and Hutter (1989) derived for the first time the depth averaged momentum and mass conservation equations obtaining one-dimensional shallow flow equations in a formulation in which Coulomb equation for basal shear resistance is assumed.

Subsequent generalizations of the Savage-Hutter approach have included extension to multidimensional avalanches (i.e. Gray et al., 1999; Denlinger and Iverson, 2001; Mangeney-Castelnau et al., 2003; McDougall and Hungr, 2004; Bouchut and Westdickenberg, 2004), incrementally advancing to a stage in which reliable application to complex phenomena appears within reach.

Whatever the numerical code is, the choice of the most appropriate constitutive law and the specification of rheological parameters are key elements to describe the flow regime.

Based on a continuum mechanics approach, RASH3D code (Pirulli, 2005; Pirulli et al., 2006) is here used to back analyse two cases of rock avalanche (Frank – Canada, 1903 and Val Pola – Italy, 1987) assuming three different constitutive laws (Frictional, Voellmy and Pouliquen).

The behaviour of the mass during propagation is analysed from two different points of view: as a function of the rheology and as a function of the morphological context in which the event moved.

2. Continuum Mechanics Approach

2.1 Governing Equations

Rock avalanches are here treated as a homogeneous and incompressible continuum. These hypotheses are grounded on the observation that depth and length of the flowing mass are usually large if compared with the characteristic dimension of the particles involved in the movement. Within these limits it becomes fundamental to find an "equivalent" fluid whose rheological properties are such that the bulk behaviour of the flowing body can simulate the expected bulk behaviour of the real landslide (Fig. 1).

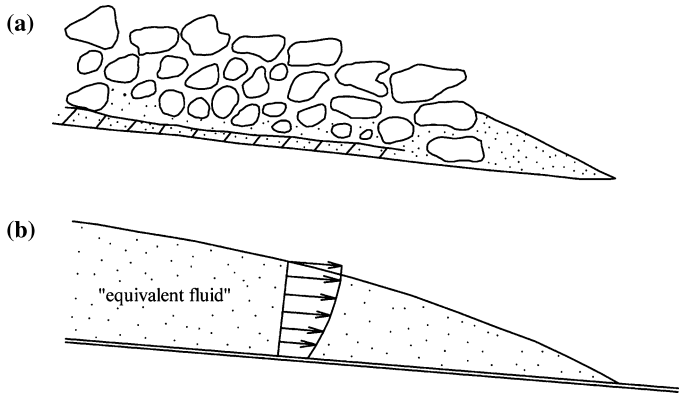

Fig. 1. (**a**) Prototype of a heterogeneous and complex moving mass; (**b**) a homogeneous ''apparent fluid'' replaces the slide mass (after Hungr, 1995).

Under these assumptions, the evolution of the avalanching mass is governed by the mass and momentum conservation laws, namely

$$\nabla \cdot \mathbf{u} = 0 \tag{1}$$

$$\rho\left(\frac{\partial \mathbf{u}}{\partial t} + \mathbf{u} \cdot \nabla \mathbf{u}\right) = \nabla \cdot \sigma + \rho \mathbf{g} \tag{2}$$

in which $\mathbf{u}(x, y, z, t) = (u(x, y, z, t), v(x, y, z, t), w(x, y, z, t))$ denotes the three-dimensional velocity vector inside the avalanche in a (x, y, z) coordinate system linked to the topography, $\sigma(x, y, z, t)$ is the Cauchy stress tensor, ρ the mass density, and $\mathbf{g}$ the vector of gravitational acceleration.

During an avalanche, the slide thickness (H) can be assumed to be much smaller than the characteristic slide length (L). Such a long-wave scaling aspect leads to depth-averaged continuum flow models governed by generalized Saint Venant equations (Savage and Hutter, 1989). This depth-averaged approach together with the assumption that most of the collisions and deformations are concentrated in the boundary layer near the bed surface (Kilburn and Sorensen, 1998) allows us to ignore changes of the mechanical behaviour within the flow.

The complex rheology of the moving material is then incorporated in a single term describing the frictional stress that develops at the interface between the flowing material and the rough surface and obeying the Coulomb-type friction law.

The Numerical Model RASH3D

Each existing model generally uses a different numerical technique to approximate the solution of the governing equations.

In a reference frame linked to the topography and in the hypothesis of isotropy of normal stresses, depth-averaged equations of mass and momentum in the x and y direction read:

$$\frac{\partial h}{\partial t} + \mathrm{div}(h\mathbf{u}) = 0 \tag{3}$$

$$\frac{\partial}{\partial t}(hu)+\frac{\partial}{\partial x}(hu^2)+\frac{\partial}{\partial y}(huv)=-\gamma_x gh-\frac{\partial}{\partial x}\left(g\gamma_z\frac{h^2}{2}\right)-\mu g\gamma_z h\frac{u}{\|\mathbf{u}\|} \tag{4}$$

$$\frac{\partial}{\partial t}(hv)+\frac{\partial}{\partial x}(huv)+\frac{\partial}{\partial y}(hv^2)=-\gamma_y gh-\frac{\partial}{\partial y}\left(g\gamma_z\frac{h^2}{2}\right)-\mu g\gamma_z h\frac{v}{\|\mathbf{u}\|} \tag{5}$$

where $\mathbf{u}=(u,v)$ denotes the depth-averaged flow velocity, h is the fluid depth, $-g(\gamma_x,\gamma_y,\gamma_z)$ the vector of gravitational acceleration, defined as the projection along the i $(=x,y,z)$ direction (Pirulli, 2005), and $\mu=\tan\delta$, where δ is the dynamic friction angle between the bed and the flowing mass.

The first term on the right-hand side of Eqs. (4) and (5) represents the driving force due to gravity, the second term is the force linked to variations in avalanche thickness and the third is the Coulomb type frictional force (Mangeney-Castelnau et al., 2003).

In RASH3D the equations of motion (3)-(4)-(5) are discretized on a general triangular grid with a finite element data structure using a particular control volume which is the median based dual cell. Fluxes of mass and momentum across cell boundaries are then computed using a finite volume method and a kinetic-type solver (Audusse et al., 2000; Bristeau et al., 2001).

2.2.1 Flow Resistance Relations

Dissipation is described in RASH3D by a Coulomb-type friction law (Mangeney-Castelnau et al., 2003) relating shear stress (τ) at the base to the normal stress (σ) at the base through a factor $\mu=\tan\delta$, involving the dynamic friction angle δ.

Due to the isotropy and incompressibility conditions, the assumed depth-averaged stress tensor is

$$\sigma=\begin{pmatrix} g\gamma_z\frac{h}{2} & 0 & 0 \\ 0 & g\gamma_z\frac{h}{2} & 0 \\ 0 & 0 & g\gamma_z\frac{h}{2} \end{pmatrix} \tag{6}$$

from which it derives the flow resistance term as quoted in Eqs. (4) and (5).

The simple *frictional rheology* ($\tau=\sigma\cdot\tan\delta$) is based on a constant friction angle, δ, which implies a constant ratio of the shear stress to the normal stress. Shear forces are independent of velocity.

Laboratory experiments carried out by Bagnold (1954) underlined that the shear stress of a granular material rapidly sheared under constant volume conditions will increase with the square of the shear strain velocity. A landslide moving on a thin, undrained layer of partially liquefied soil would thus begin its movement with a low frictional resistance, which would then increase with the square of velocity at higher speeds. To define the shear stress as a function of the velocity, the *Voellmy rheology* ($\tau=\sigma\cdot\tan\delta'+\mathbf{u}^2/\xi$) consists of a friction term ($\sigma\cdot\tan\delta'$) to describe the stopping mechanism, where the used basal friction angle δ' is typically only a fraction of the Coulomb angle δ (McDougall and Hungr, 2005), plus a turbulent term, $\mathbf{u}^2/\xi$, account-

ing for velocity-dependent friction losses, that has a great importance when the velocity of the mass is high while it vanishes at small velocities.

The turbulence coefficient ξ has the dimension of acceleration and implicitly includes the thickness of the basal layer. It is in inverse relation to the real turbulence existing in the moving mass.

Koerner (1976) and McLellan and Kaiser (1984) found that this model provide satisfactory results for rockslide avalanches in the lumped mass framework.

Instead of a turbulent term, *Pouliquen* proposed in 1999 an empirical friction coefficient $\mu = \tan\delta$ that is a function of the Froude number and the thickness h of the moving mass.

$$\mu = \tan\delta_1 + (\tan\delta_2 - \tan\delta_1)\exp\left(-\beta\frac{h}{d\cdot L}\frac{\sqrt{gh}}{\mathbf{u}}\right) \tag{7}$$

where the friction angle ranges between two values δ_1 and δ_2 depending on the values of the velocity and thickness of the flow, β is a constant function of the type of material (es. β equal to 0.136 in case of glass beads) (Pouliquen, 1999), d is the mean diameter of particles involved in the movement and L is a constant assumed equal to 10 (Heinrich et al., 2001).

The friction coefficient μ is higher for small values of the thickness and high values of the velocity. The empirical relation (7) is in fact a flow rule established for steady uniform flows over inclined plane. However it is used here as a function law for modelling real unsteady avalanches.

The presence of water in the running mass can be taken into account in RASH3D by introducing a distribution of water pressures (u) at the base of the moving mass (Pirulli, 2005).

The values of the pressures are an input data and are given through the ratio, r_u, of pore pressure to the total normal stresses at the base of the mass.

The authors are aware that this is a preliminary and rough approach to the modelling of water effect on the run out. Even though this approach needs to be improved, it has been able to reproduce some real cases of avalanches (i.e. Hungr and Evans, 1997).

3. Back Analysis Procedure

Direct field observations of catastrophic motion of avalanches are extremely difficult to make; it follows that real cases can give a limited number of information and can allow only a partial verification of theoretical models.

Laboratory experiments permit a control of both material properties and bed geometries, and thus facilitate comparison of theory with experiment.

However, a satisfactory fit of a model computation with laboratory data still does not imply that the theory is adequate to describe large scale processes in nature. Apart from the idealisations of the laboratory experiment, scale effects might falsify the conclusions. However, finding satisfactory agreement between theory and experimental results in the small scale is ''still superior to none and it constitutes a step into the direction of treating the full problem'' (Eckart et al., 2002).

In this light, before using RASH3D to the back analysis of some case histories of rock avalanche, it was widely validated through comparison with analytical solutions

and simulation of experimental laboratory tests (Mangeney et al., 2000; Pirulli, 2005; Pirulli et al., 2006).

The back analysis of a real event requires a pre- and post- event DEM, which allow the identification of the boundary of the triggering area, the geometry of the initial volume, the run out path and the deposit shape, and a detailed description of the occurred phenomenon.

Besides the above mentioned geometrical aspects, fundamental is the choice of an appropriate rheology for the type of phenomenon to be analysed. Once a rheology is assumed, a further problem is the calibration of its characteristic parameters. The higher the number of parameters required by a certain rheology, the higher the difficulty in calibrating these parameters. In some cases, however, too simple rheologies are not able to catch the main complex aspects that characterize the dynamic of a movement.

Once the geometrical data are defined and the rheology is chosen, each back analysis is carried out changing the rheological parameter using a trial-and-error procedure to obtain results that approximate in a more appropriate way on site path of propagation and deposit configuration.

4. Numerical Analyses

The three rheologies available in RASH3D and described in Sect. 2.2.1 were tested: 1) the simple frictional rheology in which only the dynamic friction angle (δ) has to be calibrated, 2) the Voellmy rheology that requires the calibration of the friction angle (δ') and the turbulence coefficient (ξ) and 3) the Pouliquen rheology in which two angles (δ_1, δ_2) plus a d parameter representative of the average granulometry of the moving mass have to be set (Sect. 2.2.1).

Since rock avalanches are recognized as mainly dry phenomena (Hungr et al., 2001), the r_u parameter that accounts for water presence has been assumed to be equal to zero in the carried out analyses. This assumption allows on the other hand reduce the number of unknown parameters to be set.

Tentative values for rheological parameters were obtained from literature. In case of Frictional and Voellmy rheologies values were extracted from Hungr and Evans (1996) where the Val Pola and the Frank events were already back-analysed with the dynamic model DAN (Hungr, 1995); while in case of Pouliquen rheology tentative

Table 1. Tentative values for rheological parameters as obtained from literature: Frictional and Voellmy values as obtained by Hungr and Evans (1996) applying the numerical code DAN to the back-analysis of both Val Pola and Frank slides; Pouliquen values as obtained by Heinrich et al. (2001) in case of the Montserrat event

SITE	Hungr and Evans (1996)			Heinrich et al. (2001)		
	Frictional	Voellmy		Pouliquen		
	δ [°]	μ ($=\tan\delta'$) [−]	ξ [m/s^2]	δ_1 [°]	δ_2 [°]	d [m]
Val Pola	16	0.1 ($=5.7°$)	500	11	25	1.5
Frank	16	0.1 ($=5.7°$)	700	11	25	1.5

values assumed by Heinrich et al. (2001) for the Montserrat avalanche were initially considered (Table 1). When the Pouliquen rheology is tested, the choice of the Montserrat event as reference case for setting the initial values of rheological parameters, in case of both Val Pola and Frank slides, was justified by both a similar volume of material involved in the movement (Val Pola $\sim 30 \times 10^6\,m^3$; Frank $\sim 30 \times 10^6\,m^3$; Montserrat $\sim 40–50 \times 10^6\,m^3$) and a good agreement among the best fit values of dynamic friction angle when the back-analysis of the three events (Frank, Val Pola, Monteserrat) is carried out assuming a simple Frictional rheology.

4.1. The Val Pola Rock Avalanche

A detailed description of the Val Pola slide is reported in Govi et al. (2002), while the information given in the present paper is set out only to define the general characteristics and the dynamic of the considered avalanche in order to better understand choices made when back analyses are carried out.

Valtellina is a valley of glacial origin located in northern Italy, near the Swiss border. The Val Pola rock avalanche (Fig. 2) moved down from the east flank of Mount Zandila, a 2936 m peak on the right side of Valtellina, and took its name after the canyon which marked the northern limit of the rock mass (Govi et al., 2002).

The period between July 15 and 28, 1987 was of particularly heavy precipitation in the Alps. A great number of flood disasters and gravitational mass movements were consequences of this meteorological coincidence. In particular, Valtellina was devastated by flooding during the first few days of the storm.

As a consequence of rainfall, beginning in the early evening of July 18, debris mixed with water, resulting in debris flows with a strong erosive power, flowed along both sides of the valley. The Val Pola torrent, a minor right side tributary of Adda river, together with a torrent from the opposite slope, placed $0.6 \times 10^6\,m^3$ debris fan across the Adda. Although mitigation measures were quickly undertaken, a lake

Fig. 2. Val Pola landslide

formed behind this blockage. By the early morning of July 28 the lake contained an estimated $0.5 \times 10^6\,m^3$.

On July 25 a 600 m long fissure opened along the base of the crown scarp of the Val Pola slide mass. Debris flows and rock falls occurred with increasing frequency over the next two days. Unloading the toe of the rock mass through landsliding and erosion along Val Pola seems to have been the key destabilizing element.

The Val Pola rock avalanche began at about 7:25 a.m. of July 28 by the detachment of an estimated rock volume of about $30 \times 10^6\,m^3$.

The slide mechanism was fully determined by major structures: a fault plane dipping at 40° formed the back scarp of the slide, another fault, coinciding with the heavily eroded Val Pola, formed the northern margin and a set of bedding joints dipping 32° traversed the slope. The resulting shape was a remarkably regular compound wedge (Smith and Hungr, 1992).

The rock mass initially shifted slowly towards the north, parallel with the dip direction of the bedding joints. Subsequently, it collapsed toward the valley. Seven men disappeared in the stream of rock fragments. A village and six hamlets, all previously evacuated, were destroyed.

The debris mass crossed the bottom of the valley, ran up the opposite slope and then parted into two arms. Part of the material in the southern arm came to rest while the other fell back, again crossed the valley and ran up the source slope (Fig. 3). Finally, a part of the mass was channelled southwards along the valley bottom. Similarly, part of the debris in the northern arm stopped, while another part ran back across the valley bottom and back up the source slope. But in this second case, a considerable

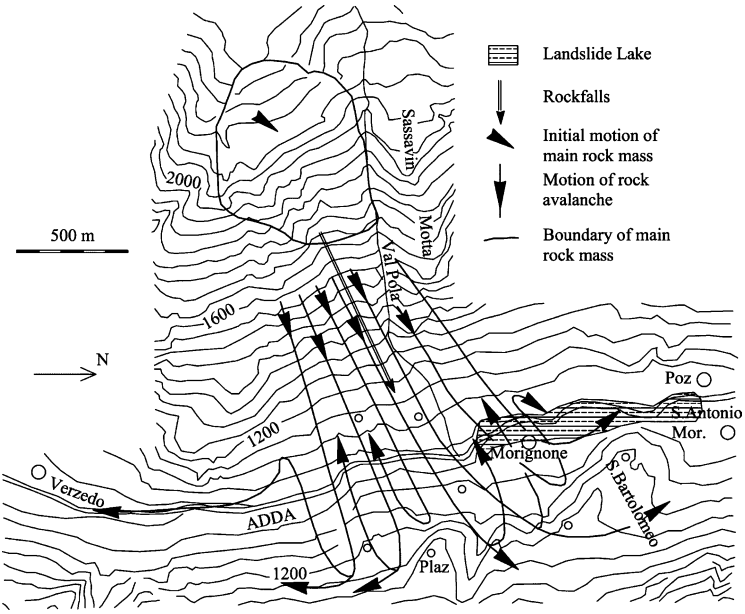

Fig. 3. State of the sites in the early morning of July 28, before the rock avalanche and rock avalanche kinematics (modified after Govi et al., 2002)

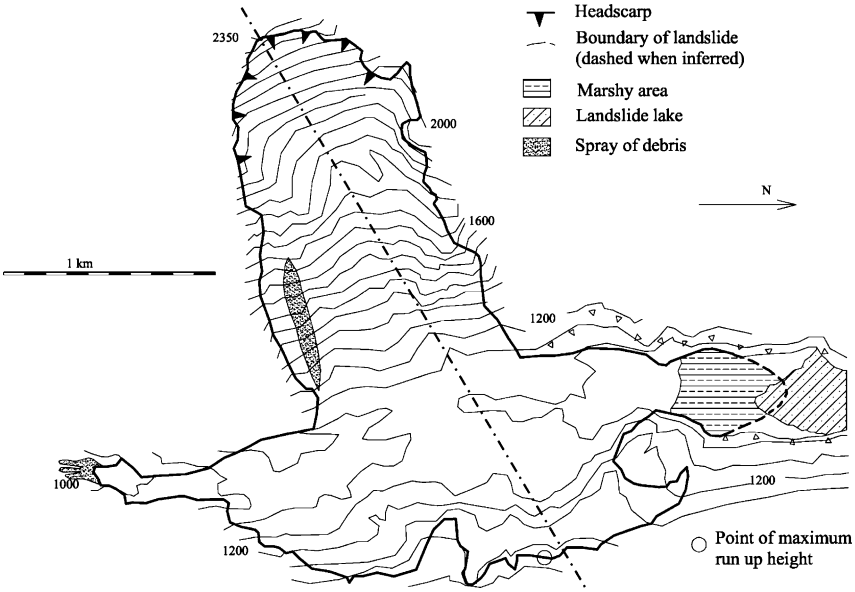

Fig. 4. Rock avalanche morphology. In the inset, subdivision by sector (after Govi et al., 2002). Dotted line gives the position of the profile considered in Fig. 5

part of the debris mass plunged into the small landslide lake formed in the previous days, and raised a huge wave of debris-water swept north along the valley bottom for more than 2 km, inundating some not evacuated villages and killing 22 people (Govi et al., 2002). When the process stopped, this arm presented a marshy area on its north side, which was followed by a new greater lake northern (Fig. 4) that can be considered as a second phase of the event much more similar to the behaviour of a debris flow.

Exposed debris consisted mainly of diorite fragments; gabbro and paragneiss were locally present (Chiesa and Azzoni, 1988). Although blocks up to 10 m and over were fairly common (some of which consisted of a conglomerate of ice and rock), the grain size of the debris ranged mostly between 0.5 m and sand size. Since about 3000 trees had been destroyed, abundant wood was scattered throughout. The maximum thickness of the accumulation was measured of about 90 m.

Taking into account that the mass descended a slope dipping about 32° along a path practically free of obstacles, it must be concluded that the initial energetic input was great. In this frame the high speed calculated by Costa (1991) of about 76–108 m/s can be considered reasonable.

4.1.1. Results of the Numerical Simulation

Before running the Val Pola back analysis with RASH3D it has been necessary to collect and organize all the available information concerning the topography of the area before and after the event. An in-depth research has allowed picking up all papers and digital information that CNR-IRPI (Italian National Research Council) and ARPA

LOMBARDIA (Regional Agency for Environmental Protection of Lombardia) have at their disposal. Collected data made it clear that a digital version of the DEM pre-event was not available. Then experts of ARPA PIEMONTE (Regional Agency for Environmental Protection of Piemonte) helped to digitize the pre-event raster information given by CNR-IRPI.

Once superposed the DEM pre-event on the DEM post-event, the boundaries of the unstable area and the triggering volume of the avalanche were obtained.

To calibrate the parameters for each of the assumed rheologies, information about the run out area shape are necessary. If the path followed by the mass along the source slope, the maximum run up of mass along the opposite slope and the south boundary of the spreading area can be defined in an enough detailed way, the north boundary of the spreading area is a little uncertain due to the behaviour assumed by the mass when it plunged into the landslide lake (Sect. 4.1).

It follows that the rock avalanche run out area to be compared with numerical results neglects both the long wave and the marshy area (Fig. 4).

A second element to be compared concerns the longitudinal profile of the final deposit (Fig. 5). As the distal point of the final deposit does not correspond to the maximum run up, it is fundamental to combine values in order to obtain a good agreement in term of run out area shape, maximum run up and final deposit profile.

Results obtained using the tentative rheological values quoted in Table 1 are represented in Fig. 6. It is observed that using these values of rheological parameters in RASH3D the run out area is overestimated in case of a Voellmy rheology and underestimated if a Pouliquen rheology is assumed. At the contrary, the Frictional values give the better approximation of the run out area shape (Fig. 6a).

In term of landslide deposit profile and maximum run up of the mass, it emerges that the distal point of the deposit is overestimated assuming both a Frictional and a

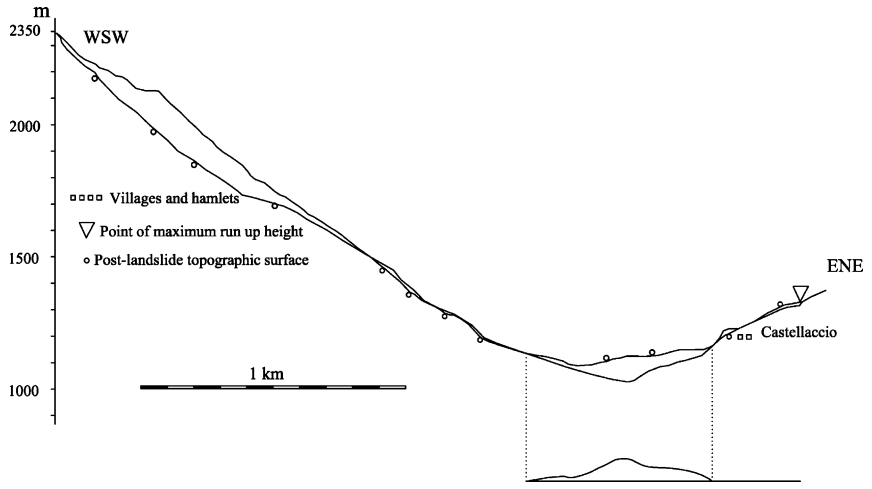

Fig. 5. Profile of the rock avalanche with pre- and post-landslide topographic surfaces. Small circles mark the post-landslide surface in the positions where incertitudines might arise. The profile WSW-ENE goes from the top of the headscarp to the point of maximum run up height uphill of Castellaccio (modified after Govi et al., 2002). The profile position is indicated in Fig. 4

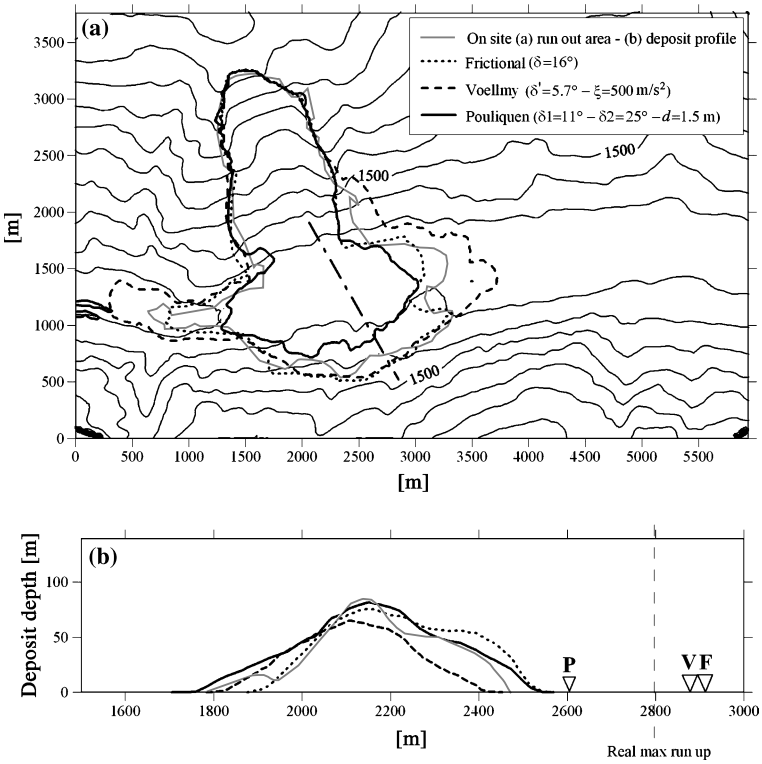

Fig. 6. Runout propagation obtained using the tentative rheological values quoted in Table 1. The profile position is the same represented in Fig. 5 and is given in plan using the long-dash dot line. The symbol ∇ gives the position of the maximum run up as a function of the assumed rheology (P: Pouliquen, V: Voellmy, F: Frictional)

Pouliquen rheology, while it is underestimated in case of a Voellmy rheology. At the contrary, in term of maximum run up, the Pouliquen rheology largely underestimates the real event behaviour while the others two rheology gives approximately the same small overestimation (Fig. 6b).

To better understand the influence of each rheological parameter, some parametric analyses were carried out starting from the above mentioned results (Table 2).

The simple frictional model was initially considered. Changing the friction angle from the initial value (Table 2, analysis *1FV*), run out area results are still acceptable if $\pm 1^\circ$ is considered (analyses *2FV* and *3FV*) while they got worse if $\pm 2^\circ$ is assumed (analyses *4FV* and *5FV*) (Fig. 7a).

Concerning the final deposit profile, it emerges that *1FV* profile (16°) is the best in term of distal point position even if the maximum run up remain incorrect (Fig. 7b).

In case of frictional rheology a dynamic friction angle of 15–16° is considered as able to give the best results in terms of run out area shape and final deposit profile. A good agreement with the value of friction angle assumed by Hungr and Evans (1996) was then confirmed.

Table 2. Parametric analyses carried out with the three assumed rheologies in case of Val Pola event. Each analysis is identified by a combination of one progressive number and two letters, the first defines the type of assumed rheology (F: Frictional, V: Voellmy, P: Pouliquen) and the second one identifies the case of back analysis considered (V: Val Pola, F: Frank)

Rheology								
Frictional		Voellmy			Pouliquen			
Analysis	δ [°]	Analysis	δ' ($\sim$arctan μ) [°]	ξ [m/s^2]	Analysis	δ_1 [°]	δ_2 [°]	d [m]
1FV	**16**	*1VV*	5.7	500	*1PV*	11	25	1.5
2FV	15	*2VV*	5.7	300	*2PV*	11	25	0.5
3FV	17	*3VV*	5.7	350	*3PV*	11	25	0.3
4FV	14	*4VV*	5.7	400	*4PV*	11	25	0.2
5FV	18	*5VV*	5.7	700	*5PV*	11	25	0.1
		6VV	5.7	1000	*6PV*	5.7	25	0.5
		7VV	6.8	500	*7PV*	11	18	0.5
		8VV	8	500	*8PV*	11	19	0.5
		9VV	8.5	500	***9PV***	**11**	**20**	**0.5**
		10VV	11	500				
		11VV	11	600				
		12VV	11	700				
		13VV	11	800				
		14VV	**11**	**1000**				

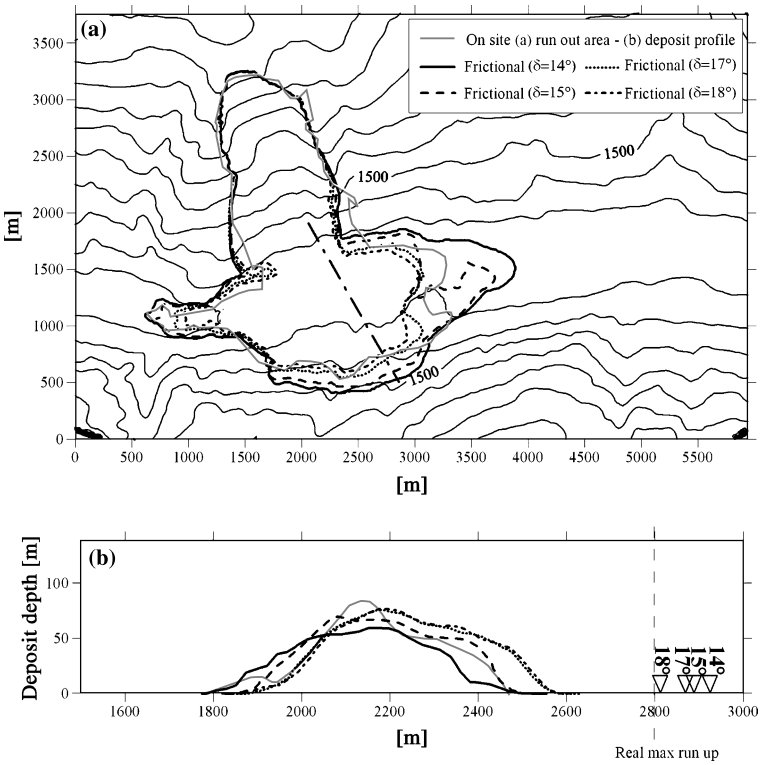

Fig. 7. Results of parametric analyses carried out assuming a frictional rheology. The profile position is the same represented in Fig. 5 and is given in plan using the long-dash dot line. The symbol ∇ gives the position of the maximum run up as a function of the assumed friction angle

In case of Voellmy rheology, the influence of each rheological parameter was investigated making three sets of parametric analysis:

(1) fixed friction angle ($d = 5.7°$) and variation of the turbulence coefficient (ξ) (Table 2, *1VV–6VV*).

(2) variation of the friction angle (d) and fixed turbulence coefficient ($\xi = 500\,\mathrm{m/s^2}$) (Table 2, *7VV–10VV*).

(3) fixed friction angle ($d = 11°$) and variation of the turbulence coefficient (ξ) (Table 2, *11VV–14VV*).

The results of the first set of analyses (1) shows that in terms of run out area shape the more satisfactory results are obtained using $\xi = 350\,\mathrm{m/s^2}$ (analysis *3VV*) but with this combination of parameters the deposit profile largely differs from the on site profile.

This lack of good results gave reason of running a second set of analyses (2) in which a constant turbulence coefficient is assumed ($\xi = 500\,\mathrm{m/s^2}$) with an increasing friction angle. The more satisfactory results are obtained using $d = 8°$ (analysis *8VV*) but the obtained deposit profile still does not correspond to the on site profile.

To obtain a good agreement both in terms of run out area and deposit profile, it was tried to move to an higher value of friction angle assuming $d = 11°$ and changing the

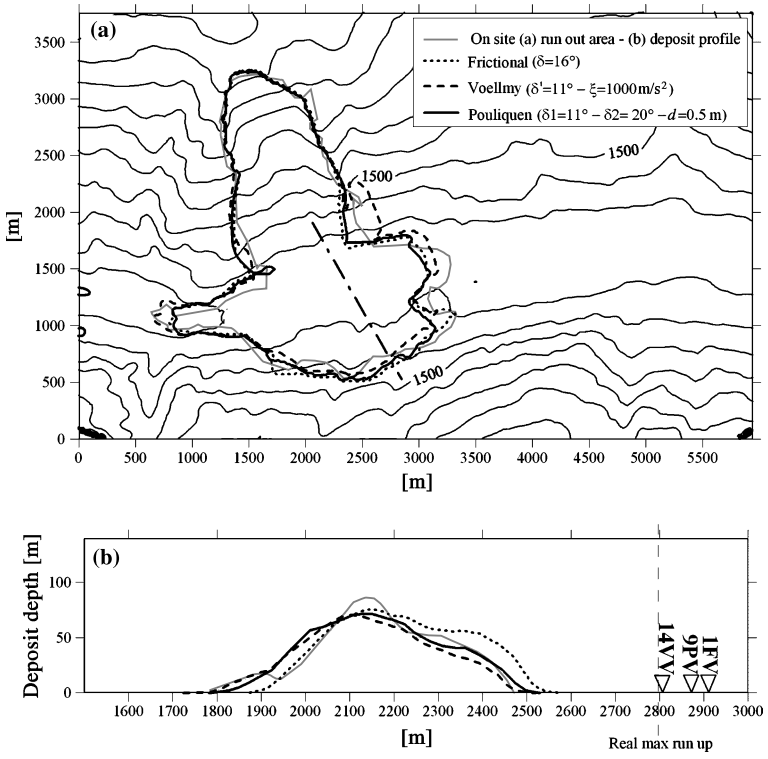

Fig. 8. Best fit results obtained in case of Voellmy and Pouliquen rheologies. The profile position is the same represented in Fig. 5 and is given in plan using the long-dash dot line. The symbol ▽ gives the position of the maximum run up as a function of the assumed rheology

turbulence coefficient (3). This assumption gave the best results with a turbulence coefficient equal to $\xi = 1000\,\mathrm{m/s^2}$ (analysis *14VV*) (Fig. 8a, b).

It can be then underlined that using a Voellmy rheology, a good correspondence in terms of run out area shape, maximum run up and final deposit profile required an higher value of friction angle ($d' = 11°$) than that proposed by Hungr and Evans (1996). Assuming lower values of friction angle any change of the turbulence coefficient was not able to give a good deposit profile.

Parametric analyses assuming Pouliquen rheology were carried out with fixing two parameters and changing the third one. Initially only the average particle diameter (d) was changed and from an initial value of $d = 1.5\,\mathrm{m}$ it was necessary to move to $d = 0.2\,\mathrm{m}$ to obtain satisfactory results (Table 2, analyses *1PV–5PV*).

Analysis *4PV* gave acceptable results in terms of both run out area and boundary of the deposit profile, but the maximum run up and the distribution of mass depth in deposit profile were widely incorrect.

Since descriptions of the Val Pola avalanche existing in literature report an average value of granulometry for material involved in the event of about 0.5 m, new analyses were carried out with Pouliquen rheology with a constant $d = 0.5\,\mathrm{m}$ and changing once δ_1 (*6PV*) and once δ_2 (*7PV–9PV*).

The best obtained fit (analysis *9PV*) gives a good agreement with on site results in terms of both run out shape, maximum run up and final deposit profile (Fig. 8a, b).

Furthermore, the $\delta_1 = 11° - \delta_2 = 20°$ interval of variation (analysis *9PV*) is considered a more acceptable range of rheological values than the range of about 20° ($\delta_1 = 5.7° - \delta_2 = 25°$) necessary to have an acceptable fit of data when δ_1 is changed (analysis *6PV*).

It can be finally stated that all the three assumed rheologies were able to reproduce the run out area and the final deposit of the Val Pola event in a satisfactory way. Nevertheless, the precision in approximating the run up of the mass was very satisfactory in case of Voellmy rheology, while an overestimate of the propagation is underlined in case of both Pouliquen and Frictional rheology (Fig. 8b).

4.2. The Frank Slide

A detailed description of the Frank slide is reported in Cruden and Krahn (1978) while information given in the present paper is set out to define the general characteristics and the dynamics of the considered avalanche in order to better understand the choices made when back analyses are carried out.

The Frank slide occurred on the morning April 29, 1903 (Fig. 9). Frank, a coal mining town of south western Alberta (Canada), located 21 km east of the border with British Columbia and 56 km north of the United States border is today an old townsite (Fig. 10). The new town of Frank is about 2 km north of the old one.

The original unstable rock mass volume is estimated at about $30 \times 10^6\,\mathrm{m^3}$ but the dimensions of the slide are not accurately known because no maps existed of the area before the slide.

The structure of Turtle Mountain was described as a monocline of Paleozoic limestones dipping at about 50°. The slide probably took place on bedding surfaces

Fig. 9. Frank Slide

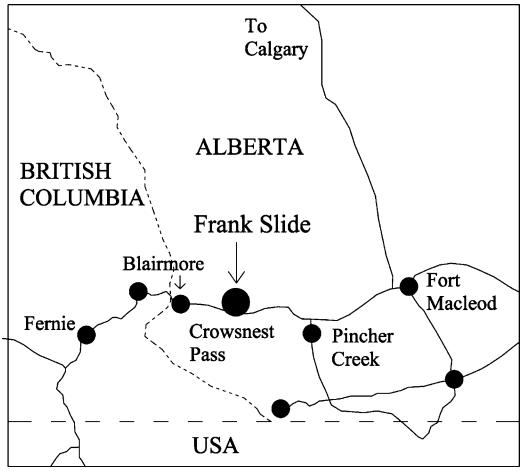

Fig. 10. Location of the Frank Slide area

with orientation of the scarp and lateral margins of the slide controlled by joints sets. A surface of rupture close to the toe of the slide followed a minor thrust above the Turtle Mountain fault.

The slide debris moved down from the east face of Turtle Mountain across the entrance of the Frank mine of the Canadian American Coal Co., the Crowsnest River, the southern end of the town of Frank, the main road from the east, and the Canadian Pacific mainline through the Crowsnest Pass (Fig. 11).

The separated rock mass seems to have been shattered by impacts against the side of the mountain during its descent, and probably long before it reached the bottom, into myriads of fragments, some of which were flung far out into the valley.

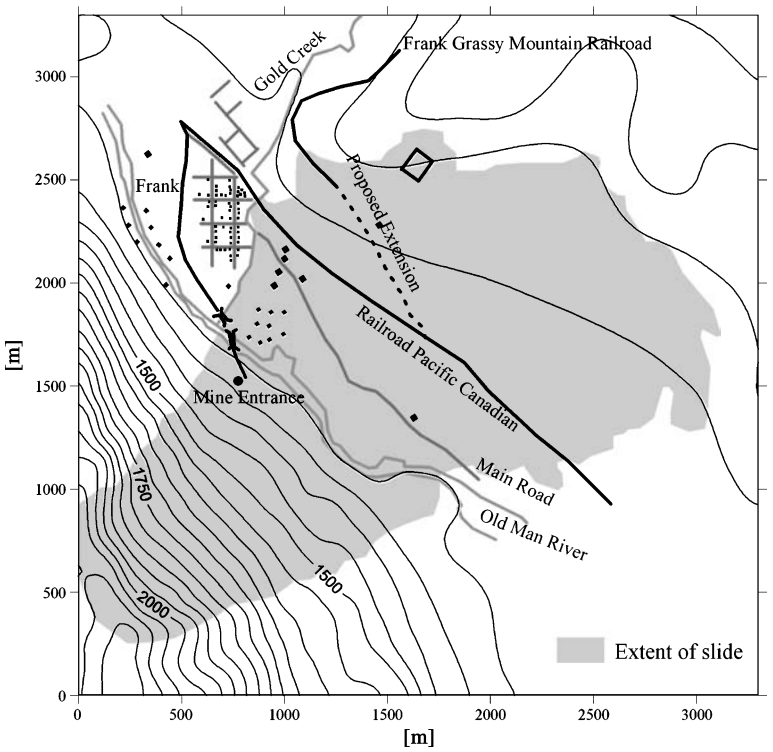

Fig. 11. Plan of the Frank Slide debris deposit with representation of elements involved in the propagation of the mass

The rock slide consists mostly of angular fragments of limestone, ranging in size from grains up to great blocks 12 m in length. Large rocks are common everywhere, especially along the central portion of the slide.

In some portions of the slide the space between the rocks are filled with finer material and a number of small mud flats are also present.

In confirmation of this, the reconstruction of the Canadian Pacific Railway line created a cut up to 16 m high across the deposit, giving a unique cross section nearly the depth of the debris. The debris shows vertical sorting. The base material is crushed limestone, mainly of sand and gravel size, and contains rounded pebbles from till or alluvial deposits on the surface of separation. The upper surface of the debris is an accumulation of large, predominantly angular boulders. Grain-size analyses demonstrate a gradual increase in grain size with height above the base of the cut. Such inverse grading with fines concentrated at the base of the debris indicates that the landslide was not fluidized by gas pore pressure (Cruden and Hungr, 1986).

In general, the great mass ploughed through the bed of the river and carrying both water and underlying sediments along with it, crossed the valley, climbed 145 m up the opposite side of the valley and finally came to rest 120 m above the valley floor with an average thickness of the debris at 13.7 m over an area of about three square kilometres.

It is difficult to reach any definite conclusion in regard to run out time, as the estimates of eye witnesses range all the way from twenty seconds to two minutes.

No estimate of the rate at which the material travelled after it broke away can be given, but as those awakened by the roar had scarcely time to do more than to rise from their beds before all was over, it must have been extremely rapid (McConnell and Brock, 1904).

The number of people killed by the slide is not known exactly, but it is given at about 70. Three-quarters of the homes in Frank were crushed like balsa wood; the people occupying the houses in the track of the slide were all swept away with it and destroyed. The track of the Canadian Pacific Railway was hopelessly buried for a distance of nearly 2000 m and the river became a lake. The entrance and buildings of the coal mining at the base of Turtle Mountain were buried. Seventeen miners trapped inside performed an astonishing self-rescue. They tunnelled upwards and broke through the surface on the face of the mountain.

For many years, Frank was the only well-described, historic example of what Varnes (1978) called a rockslide-avalanche.

Immediately after the slide an inspection was made by the Geological Survey of Canada. Their report gave a general survey of the geology of the mountain. They concluded that the slide occurred across rather than along bedding planes and believed

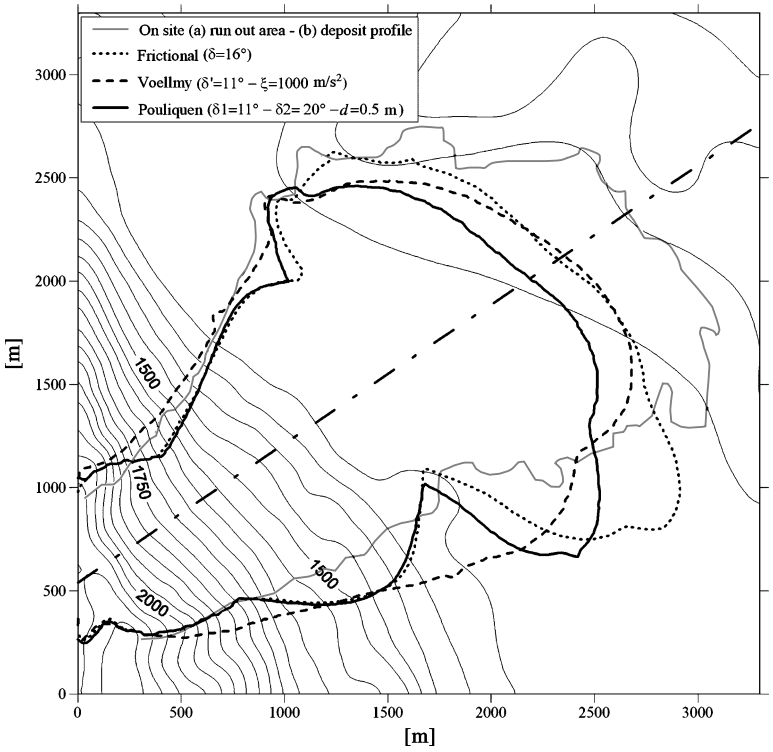

Fig. 12. Runout propagation obtained using the best fit data for rheological values as previously obtained in case of Val Pola (Table 2, analyses written in bold)

that the primary cause for the slide was to be found in the structure of the mountain. In their opinion any further danger of slides came from the north peak (Cruden and Krahn, 1978) since its structure is similar to the portion which fell away.

On the other hand, people pointed to the role of the mine as one of the causes of the catastrophe. Water action in summit cracks and severe weather conditions may have also contributed to the disaster.

4.2.1 Results of the Numerical Simulation

As previously mentioned, no before-event maps existed of the area interested by the Frank Slide but experts had been able to give a reconstruction of the topography and an estimate of volume involved together with boundaries of the triggering area using detailed digital elevation data provided by the Geological Survey of Canada as well as historical photographs and maps.

Since a profile of the existing deposit area was not at our disposal, the obtained numerical results are compared with on site data only in terms of final deposit boundaries.

In case of Frank slide, a first set of analyses was carried out starting from the best fit data previously obtained for each of the assumed rheology in case of the Val Pola event (Table 2, Analyses written in bold). Obtained results are presented in Fig. 12, it

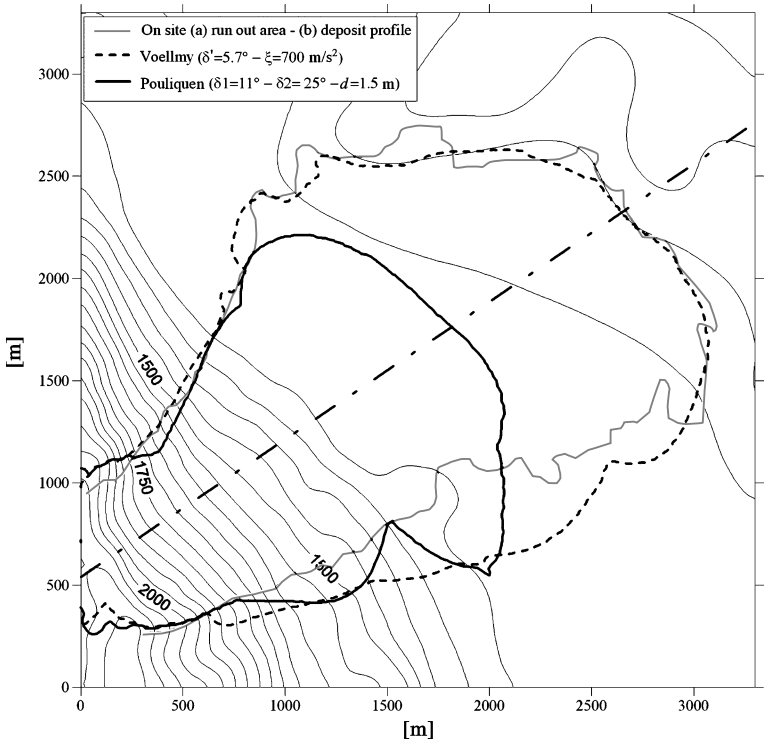

Fig. 13. Runout propagation obtained using the tentative rheological values quoted in Table 1

Table 3. Parametric analyses carried out with the three assumed rheologies in case of Frank event. Each analysis is identified by a combination of one progressive number and two letters, the first defines the type of assumed rheology (F: Frictional, V: Voellmy, P: Pouliquen) and the second one refers the case of back analysis considered (V: Val Pola, F: Frank)

Rheology								
Frictional		Voellmy			Pouliquen			
Analysis	δ [°]	Analysis	δ' ($\sim$arctan μ) [°]	ξ [m/s^2]	Analysis	δ_1 [°]	δ_2 [°]	d [m]
1FF	16	*1VF*	11	1000	*1PF*	11	20	0.5
2FF	**14**	***2VF***	**5.7**	**700**	*2PF*	11	25	1.5
		3VF	5.7	500	*3PF*	11	25	3
					4PF	11	25	1
					5PF	11	25	0.5
					6PF	11	25	0.3
					7PF	11	25	0.1
					8PF	5.7	25	1.5
					9PF	5.7	25	3
					10PF	5.7	25	0.5
					11PF	5.7	25	0.1
					12PF	5.7	14	1.5
					13PF	**5.7**	**14**	**1**
					14PF	5.7	14	0.5
					15PF	10	20	0.3
					16PF	10	18	0.3
					17PF	8	18	0.3

emerges as values obtained for the back analysis of the Val Pola widely underestimate the propagation of the mass if applied to the back analysis of the Frank slide.

A new set of analyses was then carried out assuming tentative rheological values suggested in Table 1. In this case, obtained results underline an underestimation of the propagation in case of Pouliquen rheology, while a good approximation is obtained assuming a Voellmy rheology (Fig. 13). Frictional results were the same than those presented in Fig. 12.

Starting from the simple frictional model a calibration of the rheological parameters has given good back analysis results moving to a value of the dynamic friction angle equal to 14° (Table 3, analysis *2FF*) (Fig. 14).

In case of a Voellmy rheology, to strengthen the best fit obtained using the same values assumed by Hungr and Evans, 1996, some parametric analyses were carried out but new analyses resulted less satisfactory (Table 3, analyses *3VF*).

An in deep analysis of the influence of each rheological parameter has been carried out in case of a Pouliquen rheology. A first set of analyses was obtained changing the average particle diameter, d (Table 3, analyses *2PF–7PF*). The acceptable fit is obtained when a $d = 0.1$ m is assumed (Table 3, analysis *7PF*).

In order to use a higher d-value, the angle δ_1 has been reduced to 5.7° before running new analyses in which the d-value is changed again (Table 3, analyses *8PF–11PF*). Since the best fit is again reached assuming $d = 0.1$ m (Table 3, analysis, *11PF*), the value of δ_2 has also been reduced. A value of δ_2 equal 14° gives results that are not largely influenced by the d-value (Table 3, analyses *12PF-14PF*). Further variation of δ_1, δ_2, d values did not give satisfactory results.

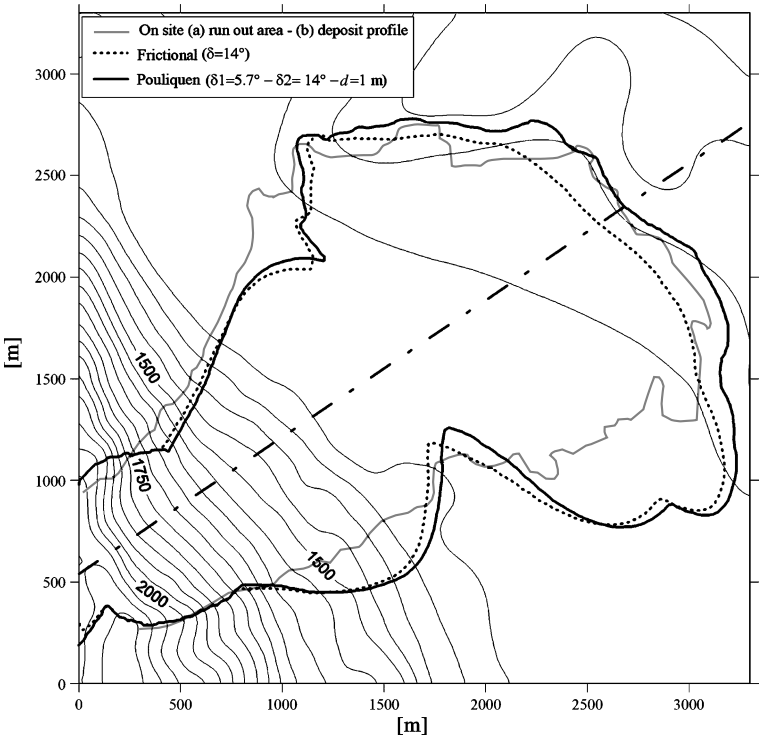

Fig. 14. Best fit results obtained in case of Frictional and Pouliquen rheologies

It can be finally stated that the analysis *13PF* has given the best approximation of the run out area shape in case of a Pouliquen rheology (Fig. 14).

The absence of a comparison in terms of mass depth distribution is due to the absence of information in on site data.

5. Discussion

The morphology of the slopes and valleys where the two analysed landslides moved (local morphology) is deeply different.

Albert Heim (1932) was probably the first to draw conclusions about the influence of local morphology and Abele (1974) distinguished some different possibilities of adaptation of the rock avalanche to local morphology. In particular, the Frank slide can be included in the category of events defined by ''spreading onto a broad valley or plain'', while in the Val Pola case ''perpendicular impact against the opposite slope'' can be assumed (Fig. 15).

Since each case has been analysed assuming three different rheologies, it was investigated the influence of the local morphology on both the deposit shape and profile for each considered rheology.

Hungr and Evans (1996) in their paper conclude that the frictional rheology tends to produce relatively short deposits, thin in the fronts and thick in the proxi-

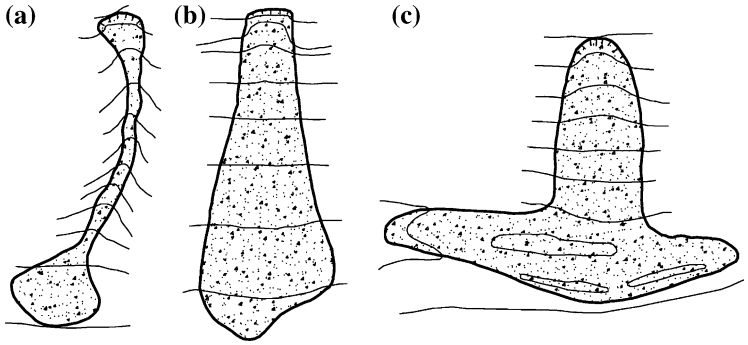

Fig. 15. Runout area shapes. (**a**) Channelling along a valley; (**b**) spreading onto a broad valley or plain; (**c**) perpendicular impact against the opposite slope (modified from Nicoletti and Sorriso-Valvo, 1991)

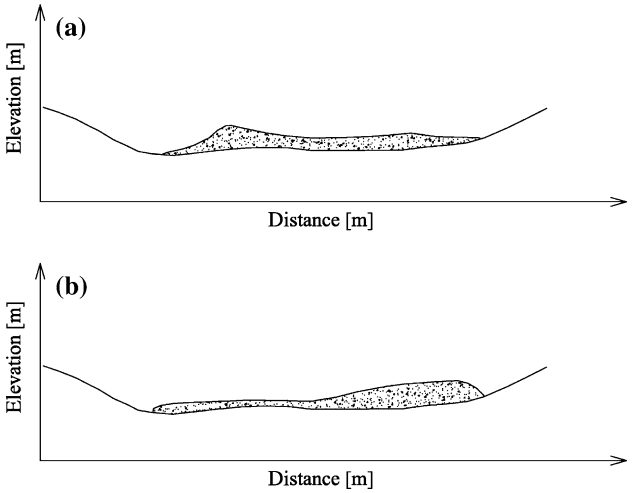

Fig. 16. Qualitative comparison of obtainable cross-sectional distribution as a function of the assumed rheology: (**a**) the Frictional rheology, (**b**) the Voellmy rheology (after Hungr et al., 2005)

mal parts; while a Voellmy rheology produces longer deposits and the opposite effect (Fig. 16).

Similarly, Mangeney-Castelnau et al. (2003) show that, for a theoretical parabolic shape of granular material flowing over an exponential topography, the simple Coulomb friction leads to granular deposit with a very different shape than that obtained using Pouliquen flow rule. The main part of the mass is located near the rear of the deposit when a simple Coulomb friction law is used whereas it is located near the front in case of Pouliquen law.

In order to check the above mentioned conditions, the calculated deposits obtained for each rheology are compared, even if the profiles of the real deposit were not available.

The distribution of the mass in the deposit area in case of Frictional and Voellmy rheologies respects indications obtained from literature both concerning the distribu-

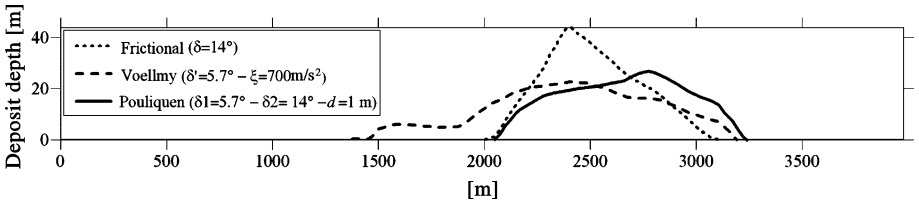

Fig. 17. Comparison of the longitudinal profile obtained with the three assumed rheologies in case of parameters values that best fit the run out area shape. The profile position is indicated in Fig. 14

tion of the mass and the longitudinal extension of the deposit. In case of a Pouliquen rheology it is observed that the deposit tend to be short, as in case of a Frictional rheology, while the distribution of the mass brings near the Voellmy profile.

Moving to the analysis of the profiles obtained in case of the Val Pola site it emerges that the existing local morphology causes, during propagation, the run up of the mass on the opposite slope respect to the triggering slope. It is observed that in this case the final deposits obtained with Voellmy, Frictional and Pouliquen rheologies are rather similar and are rather different from the profiles described in case of the Frank slide (Figs. 6b, 7b, 8b).

Indeed due to the local morphology of the analysed case, the final deposit shape can be assumed as the result of two consecutive phases: the propagation of the mass from the triggering slope and the subsequent back propagation from the reverse slope.

It can be hypothesized that in each phase the distribution of the mass is that determined by Hungr and Evans (1996) and Mangeney-Castelnau et al. (2003) as a function of the assumed rheology. In particular in case of a Frictional rheology it is the thin front that run up the opposite slope and then run back; while in case of a Voellmy rheology it is the thick front that run up the opposite slope and then run back.

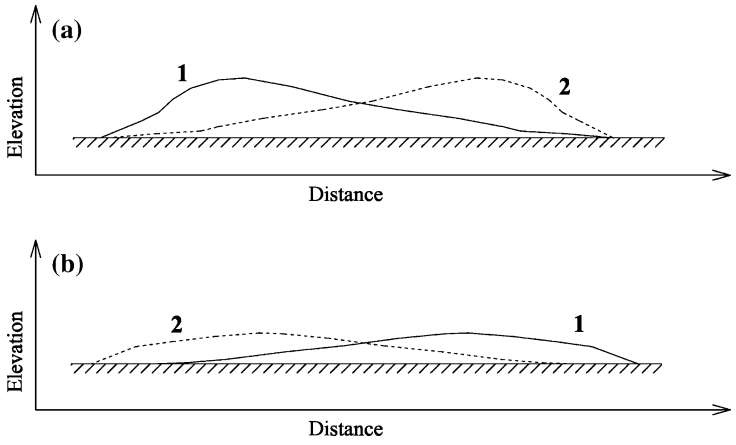

Fig. 18. Qualitative representation of the phases that could have defined the deposit profile of the Val Pola rock avalanche as a function of the assumed rheology (**a**) Frictional rheology and (**b**) Voellmy rheology. Continuous line (1) shape of the mass before run up and dotted line (2) shape of the mass following run up

In Fig. 18 it is qualitatively represented the succession of the phases that has determined the deposit in case of both Frictional and Voellmy rheology. In case of Pouliquen rheology it can be hypothesized the same mechanism assumed for a Voellmy rheology since these two rheologies give a similar distribution when a case without run up is considered (i.e. Frank slide).

6. Conclusions

The continuum mechanics model, RASH3D, developed for the run out analyses of granular material has been applied to the back analysis of two selected case histories of rock avalanches in which approximately the same volume was involved ($\sim 30 \times 10^6\,m^3$).

The carried out back analyses have allowed to calibrated in a rather accurate way the rheological parameters of each assumed rheology.

The main advantage of the *Frictional rheology* is that only one parameter has to be calibrated. This aspect is particularly important in case of prediction of a potential event.

In case of Frank slide, the observations of Hungr and Evans (1996), concerning the presence of a deposit that tends to be too short when a Frictional rheology is assumed, are confirmed. This problem does not emerge in case of the Val Pola event since the run up modify the typical deposit shape of the Frictional rheology and the final obtained deposit does not differ in a large way from that numerically calculated assuming Pouliquen or Voellmy rheology.

The best fit data for dynamic friction angle ($15 \pm 1^\circ$) are, for both the analysed cases, particularly low if compared with laboratory results or material typical frictional values. This can be considered index of heterogeneity of the involved material and of influence of water on propagation, which are not known (Mangeney-Castelnau et al., 2005; Pirulli et al., 2006).

The *Voellmy rheology* gives a satisfactory results in terms of both deposit area shape and mass distribution in case of Val Pola. This higher precision is paid by having to calibrate a second rheological parameter.

Finally, the *Pouliquen rheology* gives results that are for Val Pola as satisfactory as those obtained in case of Voellmy rheology.

The main observed disadvantage concerning the Pouliquen rheology is the difficulty in calibrating the three necessary rheological parameters. In case of prediction this can really be a drawback.

It can be finally stated that only the Frictional rheology has allowed the back-analysis of the two events assuming approximately the same value of dynamic friction angle; while the others two rheologies have required an ad hoc calibration of the parameters for having a good approximation of each case.

A second interesting aspect concerns the good correspondence between Hungr and Evans (1996) and Mangeney-Castelnau et al. (2003) observation on the distribution of the mass as a function of the assumed rheology and the distribution obtained in case of Frank slide. Further, it has also emerged how the slope morphology can determine a distribution of the mass that looses the memory of the assumed rheology and the

profile of the deposit becomes approximately the same for all the three considered rheologies. This is the case of the Val Pola where the mass run up the opposite slope.

Acknowledgements

The authors wish to acknowledge Professor Claudio Scavia for fruitful discussions and suggestions on the development of the research, Dr. Franco Godone (CNR-IRPI, Torino, Italy) and Dr. Luca Mallen (ARPA Piemonte, Torino, Italy) for their contribution to the development of the DEM of Val Pola, Dr. Scott McDougall and Professor Oldrich Hungr for having provided the data concerning the Frank slide and Dr. Marie-Odile Bristeau who put the source code of RASH3D (SHWCIN) at our disposal and helped to solve some fundamental problems.

References

Abele, G. (1974): Bergstruze in den Alpen [Landslides in the Alps]. Wissenschaftliche Alpenvereinshefte, 25, München, 230.

Audusse, E., Bristeau, M. O., Perthame, B. (2000): Kinetic schemes for Saint-Venant equations with source terms on unstructured grids. INRIA Rep. 3989, Natl. Inst. Res. Comput. Sci. and Control, Le Chesnay, France.

Bagnold, R. A. (1954): Experiments on a gravity-free dispersion of large solid spheres in a Newtonian fluid under shear. Proc. Royal Soc., London Ser. A 225, 49–63.

Bouchut, F., Westdickenberg M. (2004): Gravity driven shallow water models for arbitrary topography. Comm. Math. Sci. 2, 359–389

Bristeau, M. O., Coussin, B., Perthame, B. (2001): Boundary conditions for the shallow water equations solved by kinetic schemes. INRIA Rep. 4282, Natl. Inst. Res. Comput. Sci. and Control, Le Chesnay, France.

Chiesa, S., Azzoni, A. (1988): Esecuzione di rilievi geologici e geostrutturali sulla frana di Val Pola [A geological and geostructural field survey of the Val Pola landslide]. Bergamo, ISMES Report PROG/ASP/4284, RTF-DGM-02150, 57.

Costa, J. E. (1991): Nature, mechanics and mitigation of the Val Pola landslide, Valtellina, Italy, 1987–1988. Zeirschrift fur Geomorphologie N.F. 35, 15–38.

Cruden, D. M., Krahn, J. (1978): Frank Rockslide, Alberta, Canada. In: Voight, B. (ed.), Rockslides and Avalanches, Vol. 1, Natural Phenomena. Amsterdam: Elsevier Scientific Publishing Company. Chapter 2, 97–112.

Cruden, D. M., Hungr, O. (1986): The debris of the Frank Slide and theories of rockslide-avalanche mobility. Can. J. Earth Sci. 23, 425–432.

Davies, T. R. (1982): Spreading of rock avalanches by mechanical fluidization. Rock Mech. 15, 9–24.

Denlinger, R. P., Iverson, R. M. (2001): Flow of variably fluidized granular masses across three-dimensional terrain: 2. Numerical predictions and experimental tests. J. Geophys. Res. 106, 553–566.

Eckart, W., Faria, S., Hutter, K., Kirchner, N., Pudasaini, S., Wang, Y. (2002): Continuum description of granular materials. Spring School at the Department of Structural and Geotechnical Engineering, Politechnical Institute, Turin, Italy, 8–12 April.

Govi, M., Gullà, G., Nicoletti, P. G. (2002): Val Pola rock avalanche of July 28, 1987. In: Evans, S. G., DeGraff, J. V. (eds.), Valtellina (Central Italian Alps), in Catastrophic Landslides: Effects,

Occurrence, and Mechanisms, Review in Engineering Geology Volume XV, The Geological Society of America.

Gray, J. M. N. T., Wieland, M., Hutter, K. (1999): Gravity-driven free surface flow of granular avalanches over complex basal topography. Proc. Royal Soc. London. Ser. A, 455 (1841).

Heim, A. (1932): Bergsturz und Menschenleben. Fretz und Wasmuth, Zurich, 218. [English translation by Skermer, N. A., – Landslides and human lives, BiTech Publishers, Vancouver, 195, 1989].

Heinrich, P., Boudon, G., Komorowvski, J. C., Sparks, R. S. J., Herd, R., Voight, B. (2001): Numerical simulation of the December 1997 debris avalanche in Montserrat, Lesser Antilles. Geophys. Res. Lett. 28, 2529–2532.

Hsu, K. J. (1975): Catastrophic debris streams (sturzstroms) generated by rockfalls. Bull. Geol. Society America 86, 129–140.

Hungr, O. (1995): A model for the runout analysis of rapid flow slides, debris flows, and avalanches. Can. Geotech. J. 32, 610–623.

Hungr, O., Evans, S. G. (1996): Rock avalanche run out prediction using a dynamic model. Proc., 7th Int. Symp. Landslides, Trondheim, Norway, Vol. 1, 233–238.

Hungr, O., Evans, S. G. (1997): A dynamic model for landslides with changing mass. Proc., Int. Symp. Engineering Geology and the Environment, 23–27 June, Athens, Greece, 719–724.

Hungr, O., Evans, S. G., Bovis, M., Hutchinson, J. N. (2001): Review of the classification of landslides of the flow type. Environ. Eng. Geosci. 7, 221–238.

Hungr, O., Corominas, J., Eberhardt, E. (2005): Estimating landslide motion mechanism, travel distance and velocity. Proc., Int. Conf. Landslide Risk Management, 31 May–3 June, Vancouver, Canada, 99–128.

Kilburn, C. R. J., Sorensen, S. A. (1998): Runout lenghts of sturzstroms: The control of initial conditions and of fragment dynamics. J. Geophys. Res. 103, 17877–17884.

Koerner, H. J. (1976): Reichweite und Geschwindigkeit von Bergsturzen und fleisschneelawinen. Rock Mech. 8, 225–256.

Li, T. (1983): A mathematical model for predicting the extent of a major rockfall, Z. Geomorphol. 27, 473–482.

Mangeney, A., Heinrich, P., Roche, R. (2000): Analytical solution for testing debris avalanche numerical models. Pure Appl. Geophys. 157, 1081–1096.

Mangeney-Castelnau, A., Vilotte, J.-P., Bristeau, M. O., Perthame, B., Bouchut, F., Simeoni, C., Yernini, S. (2003): Numerical modelling of debris avalanche based on Saint-Venant equations using a kinetic scheme. J. Geophys. Res. 108 (B11), EPM 9, 1–18.

Mangeney-Castelnau, A., Bouchut, F., Vilotte, J. P., Lajeunesse, E., Aubertin, A., Pirulli, M. (2005): On the use of Saint Venant equations to simulate the spreading of a granular mass. J. Geophys. Res. 110.

McConnell, R. G., Brock, R. W. (1904): Report on the great landslide at Frank, Alberta. Department of the Interior (Canada), Annual Report 1903, part 7, 17.

McDougall, S., Hungr, O. (2004): A model for the analysis of rapid landslide runout motion across three-dimensional terrain. Can. Geotech. J. 41, 1084–1097.

McDougall, S., Hungr, O. (2005): Dynamic modelling of entrainment in rapid landslides. Can. Geotech. J. 42, 1437–1448.

McLellan, P. J., Kaiser, P. K. (1984): Application of a two-parameter model to rock avalanches in the Mackenzie Mountains. Proc., 4th Int. Symp. Landslides, Toronto, Vol. 1, 135–140.

Nicoletti, G., Sorriso-Valvo, M. (1991): Geomorphic controls of the shape and mobility of rock avalanches. Geol. Soc. Am. Bull. 103, 1365–1373.

Pirulli, M. (2005): Numerical modelling of landslide runout, a continuum mechanics approach. Ph.D. Thesis in Geotechnical Engineering, Supervisor: Prof. Scavia Claudio, Politecnico di Torino, Italy.

Pirulli, M., Bristeau, M. O., Mangeney, A., Scavia, C. (2006): The effect of earth pressure coefficient on the runout of granular material. Environ. Modell. Softw. (in press).

Pouliquen, O. (1999): Scaling laws in granular flows down rough inclined planes. Phys. Fluid. 11, 542–548.

Savage, S. B., Hutter, K. (1989): The motion of a finite mass of granular material down a rough incline. J. Fluid. Mech. 199, 177–215.

Scheidegger, A. E. (1973): On the prediction of the reach and velocity of catastrophic landslides. Rock Mech. 5, 231–236.

Smith, D., Hungr, O. (1992): Failure behaviour of large rockslide, Report to the Geological Survey of Canada and B.C. Hydro and Power Authority, DSS Contract Number 23397-9-0749/01-SZ), Thurber Engineering Ltd., Vancouver, B.C.

Varnes, D. J. (1978): Slope movement types and processes. In: Schuster, R. J., Krizek, R. J. (eds.), Landslides, analysis and control: transportation research board, National Academy of Sciences, Washington DC. Special Report 176, 11–33.

Authors' addresses: Marina Pirulli, Department of Structural and Geotechnical Engineering, Politecnico di Torino, Corso Duca degli Abruzzi, 24, 10129 Torino, Italy; e-mail: marina.pirulli@polito.it; Anne Mangeney, Equipe de Sismologie, Institut de Physique du Globe de Paris, Université Denis Diderot, 4 Place Jussieu, 75005 Paris, France; e-mail: mangeney@ipgp.jussieu.fr